Journal of *Marine Science and Engineering*

MDPI

Article

Investigation of Low-Frequency Pitch Motion Characteristics for KRISO Standard Offshore Structure (K-Semi) Moored with a Truncation Mooring System

Byeongwon Park [1,2,*], Sungjun Jung [1,2], Min-Guk Seo [1], Jinha Kim [1], Hong Gun Sung [1] and Jong-Chun Park [2]

[1] Korea Research Institute of Ships and Ocean Engineering, Daejon 34103, Republic of Korea; jungsj@kriso.re.kr (S.J.); mgseo@kriso.re.kr (M.-G.S.); jhakim@kriso.re.kr (J.K.); hgsung@kriso.re.kr (H.G.S.)
[2] Department of Naval Architecture and Ocean Engineering, Pusan National University, Busan 46241, Republic of Korea; jcpark@pusan.ac.kr
* Correspondence: bwpark@kriso.re.kr

Abstract: In this study, a model test was carried out to evaluate the station-keeping performance of Korea Research Institute of the Ships and Ocean Engineering (KRISO) standard semi-submersible, K-Semi in the Deep Ocean Engineering Basin (DOEB). The test was performed using a 1/50 scaled model with 12 mooring lines. The water depth was set to 3.2 m using a moveable bottom structure and truncated mooring lines. The dynamic behavior of the K-Semi was examined using a free decay test and regular wave as well as irregular wave tests of 1800. Large surge, heave and pitch due to drift motion from second-order effect were observed. The reason for the excessive low-frequency pitch motion is attributed to the restoring force and moment related to the mooring system as excessive surge occurred. The numerical model of K-Semi with the truncated mooring system was tuned and calibrated using model test results such as free decay and regular wave tests. Through numerical analysis, the motion characteristics of the K-Semi were compared with irregular model test results. In the case of a semi-submersible using a mooring system, it is observed that excessive pitch motion due to vertical restoring force and moment may occur when large horizontal displacement occurs. The effect of low-frequency pitch motion related to surge motion is an important factor in upwell estimation as well as second-order motion in referred DNV-GL OTG13.

Keywords: low-frequency motion; truncated mooring; mooring system; model test; semi-submersible

Citation: Park, B.; Jung, S.; Seo, M.-G.; Kim, J.; Sung, H.G.; Park, J.-C. Investigation of Low-Frequency Pitch Motion Characteristics for KRISO Standard Offshore Structure (K-Semi) Moored with a Truncation Mooring System. *J. Mar. Sci. Eng.* **2023**, *11*, 1842. https://doi.org/10.3390/jmse11101842

Academic Editor: Decheng Wan

Received: 3 August 2023
Revised: 11 September 2023
Accepted: 15 September 2023
Published: 22 September 2023

1. Introduction

Offshore structures for ocean space development are mainly divided into fixed and floating structures depending on the water depth and installation location. Jackets are fixed structures that are mainly used for ocean space development in shallow waters and are fixed to the seabed using pipes or column-shaped legs at the bottom of the structures. Jacket structures have been widely used in the development of oil fields in shallow waters. They are also widely used as a substructure for offshore wind generators based on the recent development of marine eco-friendly energy production technology.

Floating offshore structures are deployed in deep waters. A typical example of a vessel-type floating offshore structure is the floating production, storage, and offloading unit (FPSO), which is typically deployed in deep waters and areas that lack infrastructure. In addition, semi-submersibles, which have a column and pontoon structure, have the advantage of having a small waterplane area and excellent movement performance in the ocean environment; however, owing to their limited displacement, they are widely used as production facilities and drilling rigs in harsh environmental conditions rather than storage facilities in oil field development. In addition, semi-submersibles are suitable substructures

for floating offshore wind turbines; therefore, semi-submersible-type substructures for floating offshore wind turbines have been developed [1,2].

In general, the most basic requirement for the design of a floating offshore structure is the six-degrees-of-freedom dynamic behavior of the platform in the ocean environment, data on the horizontal nonlinear drift motion, relative motion, and acceleration. In particular, it is important to design and apply an appropriate mooring system so that the floating offshore structure can maintain a specific position designed for horizontal drift motion owing to external forces caused by the ocean environment, such as waves, winds, and currents. The mooring system is designed considering the installation depth, type of offshore structure, ocean environmental conditions, and positioning design criteria. The system can be categorized into chain mooring, chain combination mooring with wire or fiber rope, etc., according to the combination of mooring lines. For the design verification and performance evaluation of mooring systems for positioning offshore structures, second-order drift forces caused by different wave components were calculated and applied through potential-based numerical techniques. In addition, the performance evaluation and design verification of floating structures were performed using a model test in an offshore basin that can reproduce ocean environmental conditions by combining waves, wind, and currents.

Semi-submersible offshore structures have a deck on top of a column. The dynamic behavior under waves and the relative wave height between the wave and the deck are important design factors. A certain air gap, which is the distance between the bottom of the semi-submersible deck and the waterline, must be secured to prevent structural damage due to wave impact loads. Similarly, the relative wave height is an important factor in the design of the side shell of the column because the top of the column in the direction of wave incidence may be subjected to impact loading by waves. DNV-GL-OTG13 [3] mentions the method of calculating the air gap for structures with columns. The air gap can be calculated as a combination of wave-frequency upwells, low-frequency upwells, mean upwells, and wave elevations. Among these, the low-frequency component dynamic behavior is mainly represented as roll and pitch motion with a natural period of 40–60 s, which is caused by the Quadratic Transfer Function (QTF) of the second-order difference frequency component.

Since semi-submersibles have a small waterplane area, the restoring coefficient in the vertical direction is less than that in a ship-type structure. The restoring force of the mooring system consisting of a chain is mainly affected by the unit submerged weight of the mooring line in the catenary equation and acts in the horizontal and vertical directions at the point connected to the platform. Therefore, the mooring system is designed to maintain its position by increasing the restoring forces of the mooring line acting on the platform as the distance from the reference point is increased. Thus, the vertical motion of the semi-submersible is influenced by the mooring system as the platform drifts away from its original location.

Nam et al. [4] conducted a wave measurement experiment considering the floating body motion of K-Semi using two types of relative wave gauges (resistive and capacitive) attached to the floating body in the ocean engineering basin of the Korea Institute of Shipbuilding and Offshore Engineering. They calculated the relative wave height using the method presented in DNV-GL-OTG13 [3] and estimated the asymmetric factor and extreme upwell. Kim et al. [5] presented the results of a model test on the nonlinear run-up characteristics of a semi-submersible offshore structure as a function of wave height during a regular wave under two draft conditions. It was found that semi-submersible offshore structures exhibited nonlinear run-up characteristics in short periods combined with low draft conditions when evaluating the air gap of the semi-submersible.

Reig et al. [6] proposed a technique for fast QTF calculations using the slender body theory and model truncation for the column structure of a semi-submersible. For the semi-submersible substructure of the DTU 10 MW wind turbine, Cao et al. [7] studied the dynamic behavior due to second-order wave component using the full QTF and Newman

approximation and found that the full QTF provided relatively accurate results for the low-frequency pitch motion.

Jung et al. [8] investigated the effects of a truncated mooring system on the restoring force under limited water depth conditions through model tests of two truncated mooring systems in the deep-ocean engineering basin of the Korea Institute of Shipbuilding and Offshore Engineering (KRISO). It mentions that two types of truncated mooring were designed according to the water depth conditions that can simulate the original mooring system and applied to the model test and that similar results were obtained compared to the original mooring system even when truncated mooring was applied. Nam et al. [9] investigated the effects of the wave drift and viscous drag forces on the horizontal drift motion of a K-semi and the effects of surge and pitch motion due to the mooring system configuration applied in the model test. It also examines the effects of surge and pitch coupling via numerical analysis under soft mooring conditions as well as under truncated mooring and confirms that the effect of pitch behavior due to surge behavior is relatively small under soft mooring conditions. Ghafari and Dardel [10] investigated the motion characteristics of a semi-submersible with and without a mooring system through frequency and time–domain analyses as well as model tests. Kim et al. [11] performed a time–domain coupled analysis of a mooring system and platform using the linear spring method and the nonlinear finite element method (FEM) and found that the nonlinear method yielded relatively better results. It is also stated in [11] that the large weight of the mooring or large wave drifting force had a significant influence on the surge and pitch-coupled motion caused by the mooring system. Matos et al. [12] confirmed the occurrence of long-period roll and pitch motions caused by second wave forces in a P-52 semi-submersible deployed in the Campos Basin, which are sometimes larger than the wave frequency motions.

Molins et al. [13] suggest the use of truncated mooring systems to evaluate original mooring systems, which is an alternative when there is insufficient space in test facilities. For a mooring system applied to Windcrete, a new concrete spa platform for floating offshore wind turbines (FOWTs) has been developed. An algorithm was developed and applied to optimise the design of a scaled truncated mooring system using lines of different weights, and it was found that the static restoring force of the truncated mooring system matched well with the original mooring system. Ferreira et al. [14] mentioned the problem of mooring system similarity due to the water depth condition in the model test and proposed a design optimisation technique to find the ideal truncated design considering dynamic effects. The calibration method was applied to adjust the design parameters to optimally fit the truncated mooring system to the full-depth mooring system in order to minimise the differences in motion response and tension for two mooring systems, catenary and semi-taut. In addition, the optimum truncated design was carried out for various wave conditions through dynamic simulation, and it was found that the truncated and full-depth mooring designs yielded equivalent results in both cases. Kim et al. [15] mention a technique for designing a truncated mooring system to suit basin conditions, as a full-depth mooring system is difficult to apply directly to a model test due to the limitations of basin size and water depth conditions. Wang et al. [16] designed and conducted a station-keeping performance evaluation of truncated mooring systems at two water depths, 736 m and 460 m, for FPSO with a turret mooring system in 914 m of water depth. The truncated mooring system was designed to be as similar as possible to the original mooring system in terms of static and dynamic characteristics, dynamic characteristics of the floater and tension characteristics of each mooring line. The truncation factor was defined as the ratio of the original mooring system to the truncated mooring system in water conditions, and the results showed relatively good agreement with the original mooring system results when the truncation factor was large, which is 736 m water depth condition.

Waals and Dijk [17] discuss the design technique of a truncated mooring system for performing mooring system model tests. The design of a truncated mooring system is carried out in two steps to design a truncated mooring system similar to a full-depth mooring system under static and dynamic conditions. First, the optimum design conditions are found for static loading conditions with variations in mooring length, weight in water and axial stiffness, and then the optimum design conditions are found for dynamic loading conditions with variations in mooring weight and diameter. It is also mentioned that for floating platforms with lower vertical restoring coefficient, it is necessary to consider the coupling behavior due to the mooring system. This is because the pre-tension angle changes of the mooring line when moving in the surge direction, and this induces a pitch moment. Li et al. [18] investigated the effect of the horizontal and vertical stiffness of the mooring system on the estimation of the air gap of a semi-submersible. In the model test, three wave probes were installed to measure the relative wave height and the air gap was estimated. The results of the model test showed that the effect of horizontal stiffness on the air gap was significant. The effect of vertical stiffness was investigated using the ratio of the heave restoring coefficient of the floater to the vertical stiffness of the mooring. The effect of air gap was insignificant when the vertical stiffness of the mooring was small compared to the heave restoring coefficient, but the effect of air gap was significant when the vertical stiffness of the mooring was large compared to the heave restoring coefficient.

This research investigates the coupling effects of surge and pitch motions of a moored semi-submersible used for offshore development. Column structures such as semi-submersibles are characterized by a small waterplane area, resulting in small heave, roll and pitch restoring coefficients and a long natural period of each motion. In the case of roll and pitch motions with long natural periods, such as a semi-submersible, the pitch motion caused by the 2nd order component is important in addition to the wave frequency component. In addition, the pitch motion of a semi-submersible is inevitably affected by the vertical force of the mooring system, and the greater the surge motion, the greater the force of the mooring system and, therefore, the greater the effect on the pitch motion.

In this study, K-Semi, a KRISO standard offshore structure, was used as a target offshore structure for model testing to evaluate the dynamic behavior of K-Semi in a truncated mooring system in the Deep Ocean Engineering Basin of KRISO, Busan, and the results were compared with frequency and time domain numerical analyses. Model tests and numerical analyses were used to investigate the wave frequency and low-frequency motions caused by the second-order wave force of the K-Semi and the low-frequency pitch motion of the semi-submersible influenced by the mooring system as the platform drifted away. The three main components (wave frequency motion, 2nd order motion and low-frequency motion due to surge drift motion) of the pitch motion appear through spectrum analysis of the pitch time series measured in the model test. These pitch motions coupled with surge motions can cause higher relative wave heights on the semi-submersible. The relative wave height on an offshore structure is a major factor that can cause impact loads on the structure, so it should be treated as an important issue.

2. Test Model

2.1. Hull Model

In this study, K-Semi, a standard offshore structure at KRISO, was used as the reference model. K-Semi is an open-standard offshore platform model for research and technology development purposes, and its hull shape is shown in Figure 1. K-Semi has two loading conditions for operation and survival. In this study, the survival condition, which is an extreme condition, was considered. The main characteristics of the KRISO standard offshore structure, K-Semi, used in the model test are listed in Table 1. A 1:50 scale model used for the model test is shown in Figure 2.

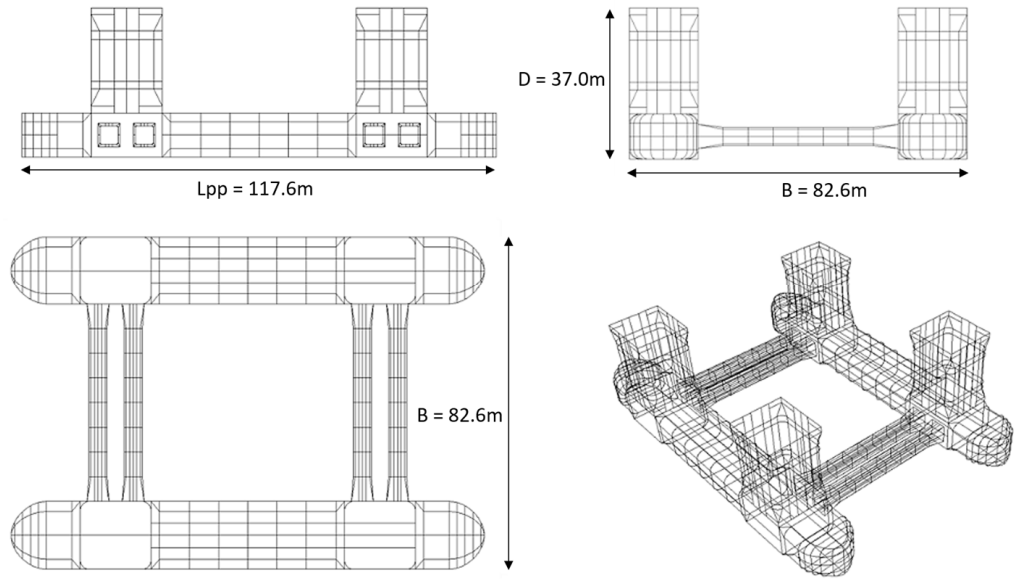

Figure 1. Hull form of KRISO Semi-Submersible (K-Semi).

Table 1. Particulars of K-Semi.

Scale		Unit	Full (1:1)	Model (1:50)
Loading Condition			Survival Condition	
Lpp		m	117.6	2.352
B		m	82.6	0.923
D		m	37.0	0.74
T, midship		m	19.0	0.38
Displacement		m^3	56,033.9	0.4483
Weight		kg	56,033,900	448.3
C.O.G. from AP, Center, Base	X	m	58.8	1.176
	Y	m	0.0	0.0
	Z	m	26.9	0.538
KMt		m	30.5	0.61
KMl		m	30.5	0.61
Kxx		m	33.0	0.66
Ky		m	33.0	0.66
Kzz		m	33.0	0.66
GMt		m	3.631	0.0726
GMl		m	3.623	0.0725
Resonance Period	Heave	s	20.61	2.915
	Roll	s	50.37	7.124
	Pitch	s	48.62	6.876

Figure 2. Manufactured test model of K-semi with scale ratio 1/50.

2.2. Mooring System Model

The radial mooring system for maintaining the position of K-Semi consists of 12 chain moorings. The designed depth of the K-semi was 300 m. Based on Froude's law, the water depth in the test model is required to be 6 m. In this model test, the water depth of the Deep Ocean Engineering Basin (DOEB) was set to 3.2 m. Here, the geometric similarity of the original mooring system could not be satisfied for this water depth. Therefore, a truncated mooring system was designed and implemented to provide a pre-tension tension and restoring force in the horizontal offset condition.

The truncated mooring system was designed to have the equivalent horizontal restoring force and pre-tension of the original mooring system under offshore basin conditions. The truncated mooring system design technique was adapted from the methods presented by Kim et al. [15] and Waalin and Dijk [17]. In this study, the design factors of the truncated mooring system are considered in terms of mooring length, weight in water and axial stiffness, and the truncated mooring is designed to approximate the pre-tensioning and horizontal restoring to surge offset of the original mooring system. The initial range of design factors was calculated based on the truncation factor using the ratio of the original water depth and the basin water depth for the truncation, and the surge offset and pre-tension restoring forces were evaluated via numerical analysis. Based on the evaluation results, the specifications of the truncated mooring system were selected by modifying the length, water weight and axial stiffness, if necessary, through comparison with the original mooring system. However, in order to apply the designed truncated mooring system to the model test, it is necessary to modify it to make it suitable for the model test, so the final specifications of the truncated mooring system were determined by considering the feasibility of the actual model and implementation. Figure 3 summarizes the design process of the truncated mooring system used in this study. Additionally, the specifications of the original and truncated mooring system are listed in Table 2.

The layouts and geometries of the original and designed truncated mooring systems are compared in Figure 4. The original mooring system had a paid-out length of 1700 m and an anchor point approximately 1614 m away from the fairlead. The truncated mooring system for the model test had a paid-out length of 672 m and was anchored at a point 600 m away from the model fairlead. This implies that the anchor was located 12.0 m away from the model, considering the scaling law. The truncated mooring line utilized in the model test is shown in Figure 5. In its construction, a chain was employed as the base material and weights were placed at equal intervals to meet the weight per unit length condition.

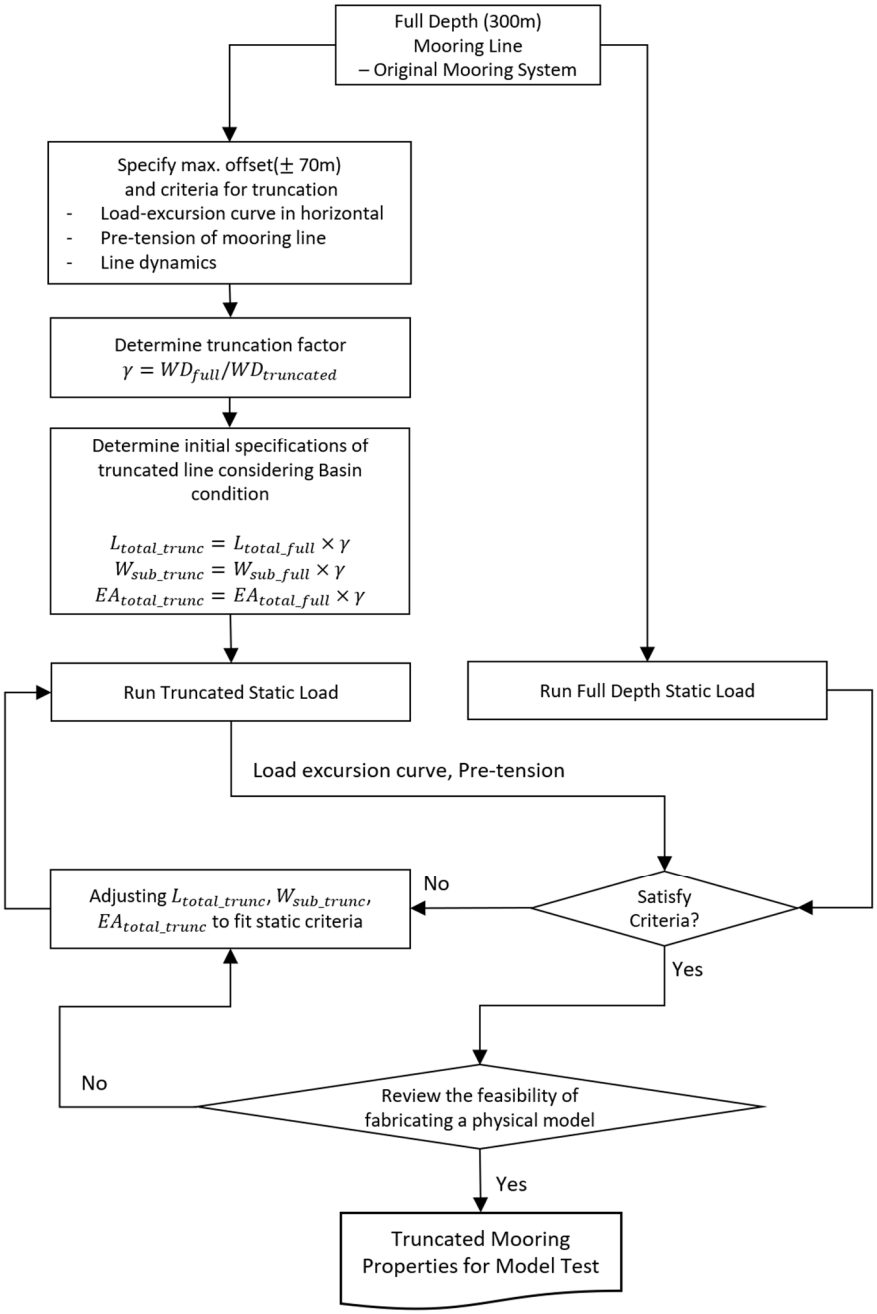

Figure 3. Design strategy of truncated mooring lines for model test.

Table 2. Specification of mooring line for original and truncated mooring system.

Item	Unit	Original Mooring	Truncated Mooring					
		Full Scale	Full Scale			Model Scale		
		Chain	Chain	Spring	Loadcell	Chain	Spring	Loadcell
Diameter	[m]	0.084	0.1621	0.153	0.1921	0.0032	0.003	0.0038
Pre-Tension	[kN]	1342		1335.8			0.0107	
Length	[m]	1700	644.15	25	2.85	12.883	0.5	0.057
Mass in water	[kg/m]	135	499.7	445	701.8	0.2	0.178	0.281
Axial stiffness	[kN]	6.34×10^5	2.36×10^6	7357.5	3.32×10^6	1.89×10^1	5.89×10^{-2}	2.65×10^1

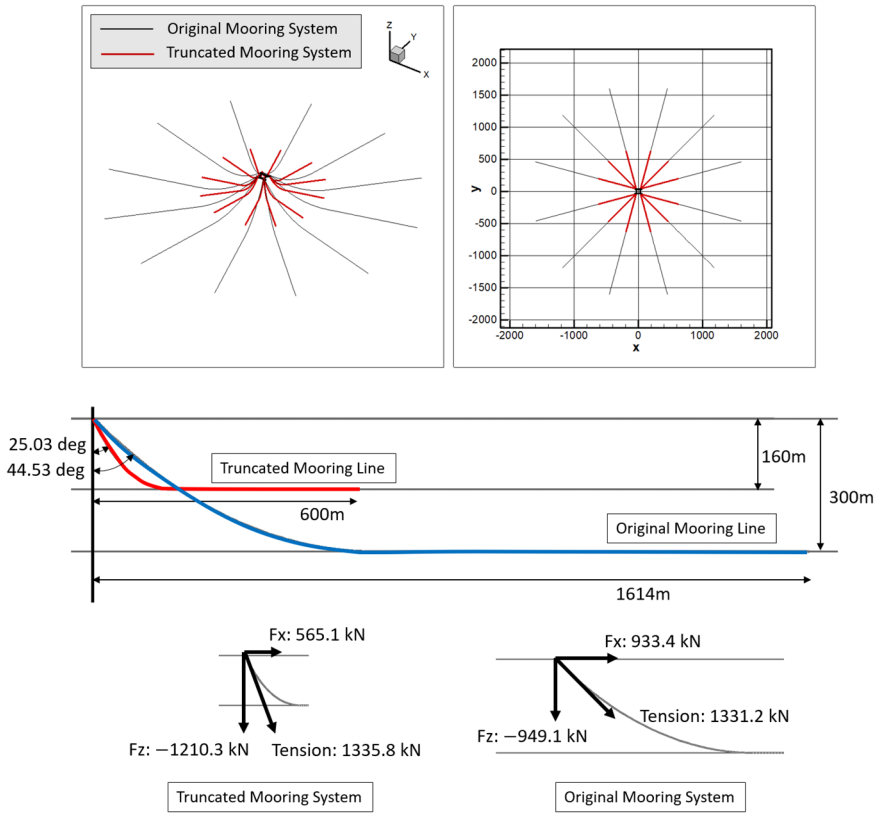

Figure 4. Layout of mooring system and configuration of mooring line of original and truncated.

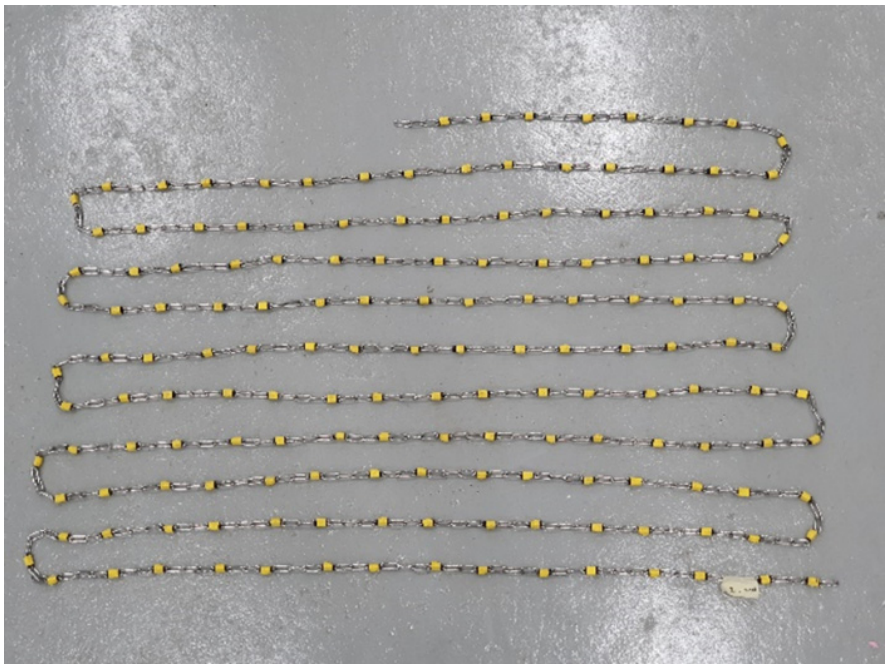

Figure 5. Mooring line of truncated mooring system for model test.

2.3. Numerical Model

Numerical analyses were carried out to investigate the motion characteristics of K-Semi. Frequency–domain analysis and time–domain analysis were carried out using the in-house program AdFLOW and OrcaFlex (version 11.3d), respectively [19,20].

Figure 6 shows a higher-order panel model used for the AdFlow analysis. The model consists of nine nodes, forming a panel structure below the waterline. Frequency–domain analysis was carried out to obtain the hydrodynamic coefficients of K-Semi, which were then utilized to obtain the Response Amplitude Operator (RAO) and QTF.

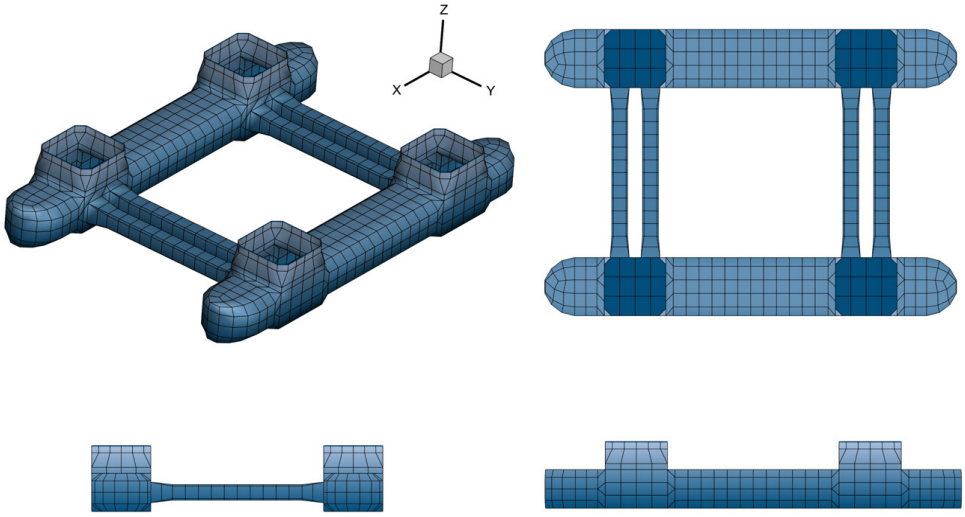

Figure 6. Panel modeling of K-semi for AdFlow analysis.

Figure 7 shows the numerical analysis models for both the original and truncated mooring systems using OrcaFlex for time–domain analysis. Data such as hydrodynamic coefficients and QTF for the floating body calculated by AdFlow were input to OrcaFlex for the time–domain analysis. The mooring characteristics of each system in the time domain simulation were modelled using the design characteristics of the original and truncated moorings. The numerical model was calibrated utilizing the results of the mooring system restoring force in the horizontal offset condition, the free decay test, and the regular wave model test to calibrate the damping coefficients and obtain results similar to those of the model test. The motion performance of K-semi under irregular wave conditions was analyzed and compared with the model test results.

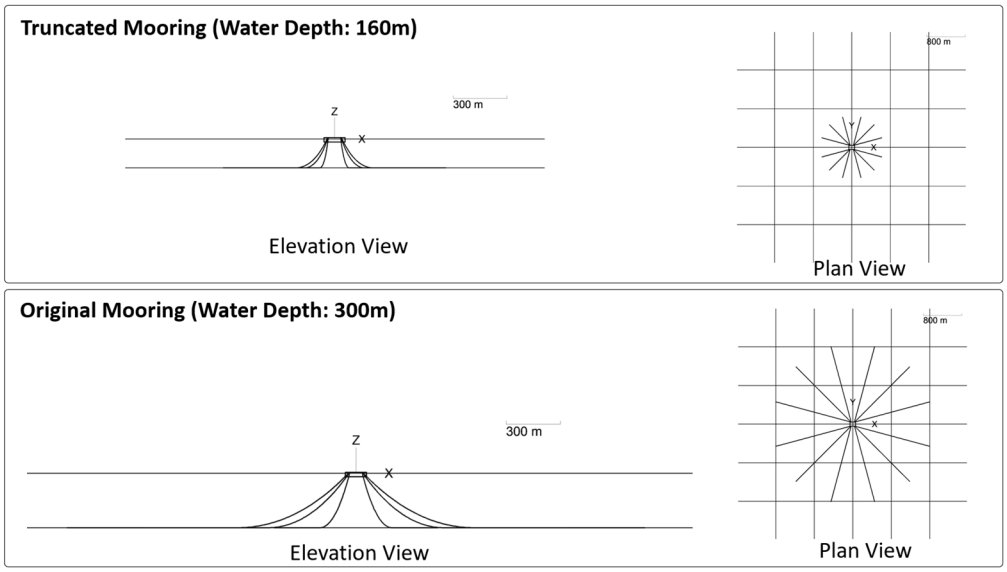

Figure 7. Modeling of K-semi with original and truncated mooring system for time domain simulation in OrcaFlex.

3. Model Test Conditions

3.1. Layout for Model Test

The K-Semi model and truncated mooring system were placed in the DOEB of the KRISO, as shown in Figure 8. Figure 9 shows the K-Semi model installed in the basin. The K-Semi was placed at the center of the basin as the initial position, and the end of the mooring line was installed at the anchor point of the truncated mooring system. Three wave gauges were installed for wave calibration. The wave gauge at the K-Semi location was removed when the model was installed in the main tests. The six-degrees-of-freedom motion of the K-Semi was measured using the Qualisys optical measurement system, which is manufactured by Qualisys AB in Sweden. A single-axis load cell was installed on each mooring line to measure the tension in the mooring system.

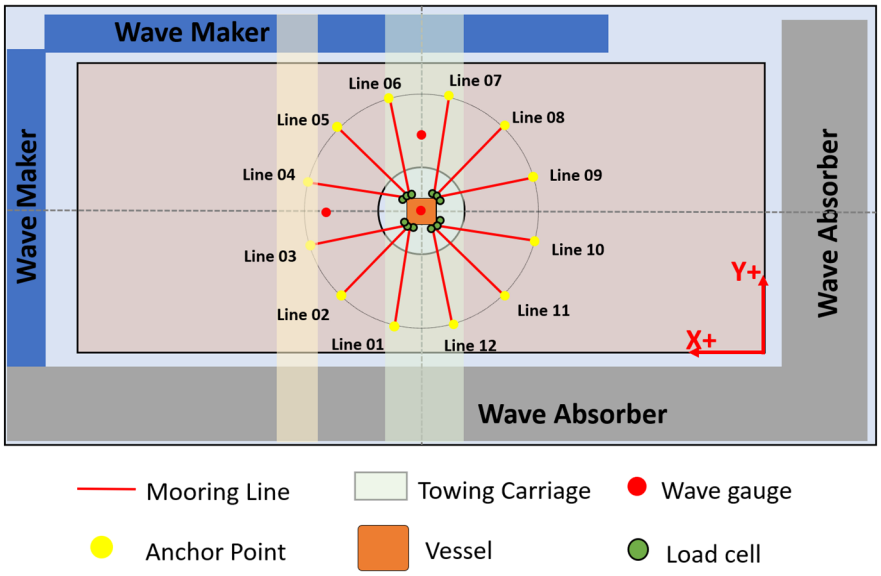

Figure 8. Layout of K-Semi and mooring system in basin.

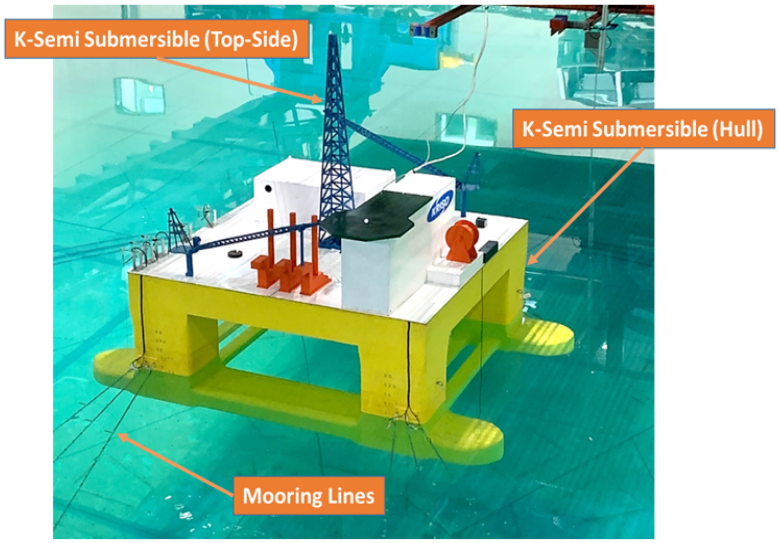

Figure 9. Snapshot of K-semi and mooring system for model test.

3.2. Restoring Comparison of Mooring System

To verify that the restoring force of the fabricated truncated mooring system was accurate, a pull-out test was performed according to the stern offset of the K-Semi. In the pull-out test, a line was attached to the stern of the K-semi and various loads were applied

at the end of the line using unit weights. The displacement of the K-Semi was measured versus the applied load, and the relationships between them were obtained.

The restoring force results derived from the numerical analysis (original mooring depth of 300 m, truncated mooring depth of 160 m) and the restoring force results from the pull-out test of the truncated mooring system applied to the model test are shown in Figure 10, confirming that the restoring force in the surge direction of the model mooring system is configured to match the design value well.

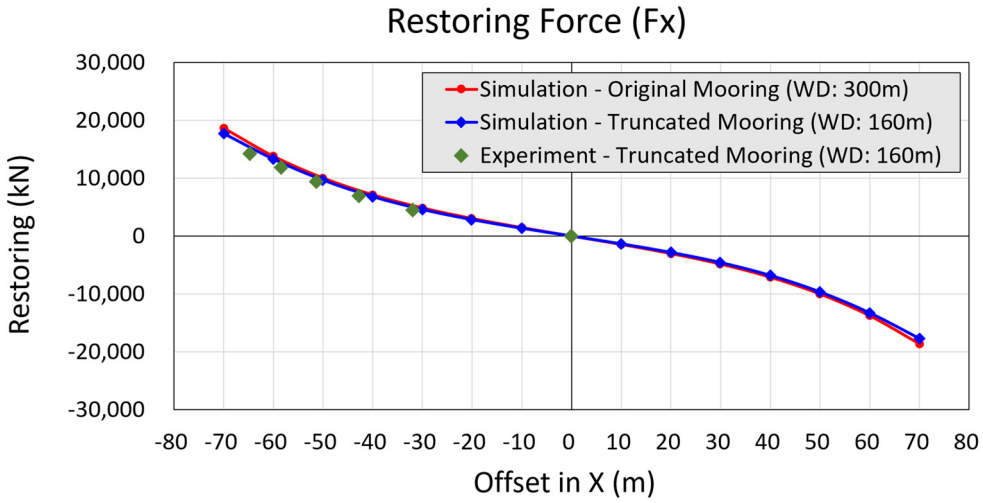

Figure 10. Comparison of restoring force results from pull out test in surge direction.

Since the main purpose of the mooring system was to generate restoring forces in the horizontal direction to maintain the position of the floating body, a truncated mooring system was designed such that the pre-tension and horizontal restoring forces were the same as those of the original mooring system. Numerical analysis was carried out to investigate the load components acting on the mooring line as the K-Semi moved in the heave direction. The restoring forces in the heave motion of the original and truncated mooring systems are shown in Figure 11, and the restoring moments in the pitch motion are shown in Figure 12. As can be seen from these two figures, the pitch restoring moment increases sharply with increasing offset of the K-semi. The restoring force of the heave motion and the restoring moment of the pitch motion are found to be much larger in the truncated mooring system than in the original mooring system. As mentioned in Section 1, the semi-submersible type of offshore structure has a small waterplane area. Therefore, the motion response of a K-semi with a small pitch restoring coefficient can be affected by large restoring moments induced by the mooring system when low-frequency drift motion occurs in the surge direction. Because heave and pitch motions are considered in the relative wave calculation of DNV-GL-OTG13 [3], they may affect the assessment of the hull impact load due to the relative wave. Hence, strict consideration of heave and pitch motions, especially for the low-frequency component, is required.

3.3. Environmental Condition for Model Test

In this study, a model test was conducted to investigate the motion response of K-Semi connected to a truncated mooring system. Free decay tests were performed to identify the six degrees of freedom motion characteristics of the K-Semi model, and the RAO was investigated using a regular wave test at an incident angle of 180°. In addition, the motion response characteristics of the K-semi in horizontal drift motion were evaluated via an irregular wave test under survival environment conditions with an incident angle of 180°. In addition, the dynamic behavior characteristics of K-Semi were studied by analyzing the motion time series.

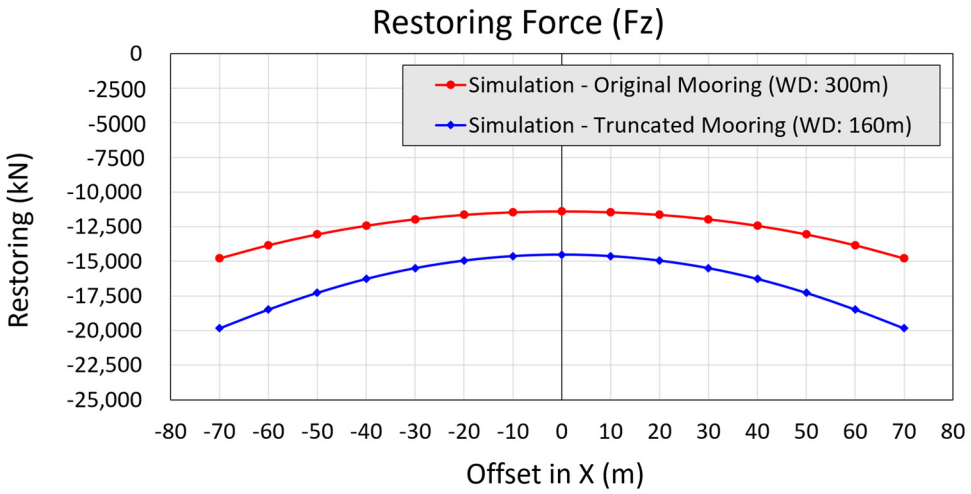

Figure 11. Comparison of restoring force results from pull out test in heave direction.

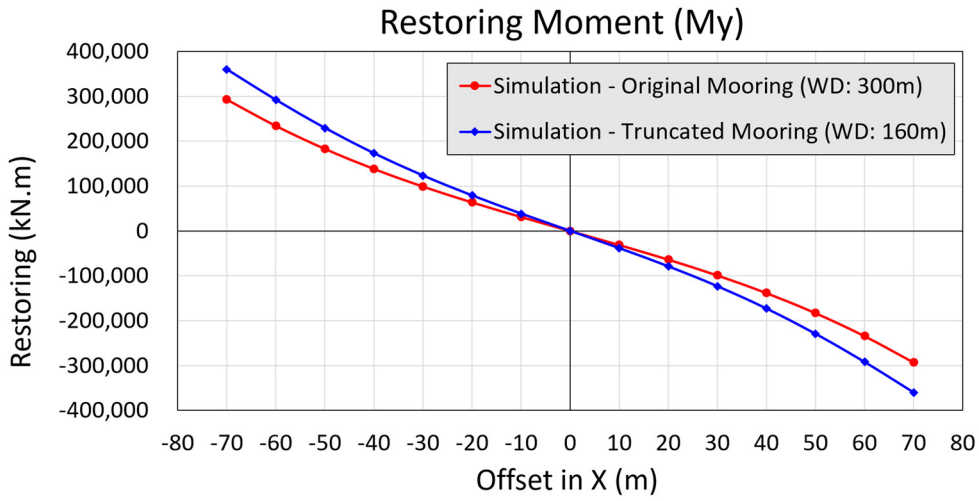

Figure 12. Comparison of restoring moment results from pull out test in pitch direction.

Table 3 summarizes the test conditions used in the study. The JONSWAP Spectrum was used for the irregular wave condition, and a gamma value of 3.3 was applied.

Table 3. Test matrix for model test in basin.

Test No.	Test Type	T, Tp	H, Hs	beta
		[s]	[m]	(deg)
1	Decay Test	6 DOF with truncated mooring		
2	Regular Wave	14, 15, 16, 18, 19, 19.7, 20.3, 21, 22, 23	5.0	180
3	Irregular Wave	10.64	7.5	180

4. Comparison Result between Model Test and Analysis

4.1. Free Decay Test

To investigate the motion characteristics of the K-Semi connected to the truncated mooring system, a decay test and regular wave model test were performed to measure the six-degrees-of-freedom motion of the K-semi.

A six-degrees-of-freedom motion was performed in the decay test, and the results of the surge motion are shown in Figure 13. The pitch motion results, which are of interest in this study, are shown in Figure 14. These are normalized with respect to the initial values

and are compared with the results of the numerical analysis. In K–Semi's numerical model, the damping coefficients for the floating body were chosen such that they had the same motion characteristics as in the experimental results. The initial damping coefficients were estimated using the free-decay model test to determine the linear and nonlinear damping coefficients. These were then incorporated into the numerical analysis. To ensure accurate representation, the model test time series was used, and adjustments were made through the trial-error method until a match was achieved. The free decay analysis results are similar to those of the model test for the pitch motion time series. However, variations in the periods of the surge motion are observed. It is believed that this is due to the difference in the added mass of the mooring line considered in the time domain analysis model and the influence of the low-frequency motion caused by the fluid drag component of the floating body and mooring, which is not considered in this study [9].

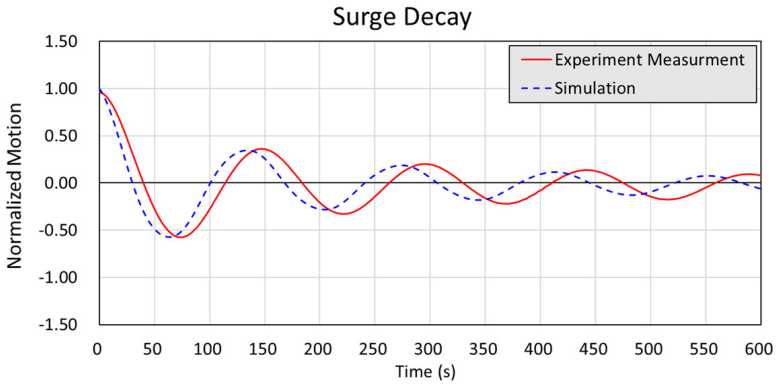

Figure 13. Comparison of time series between experiment and simulation result for surge decay test.

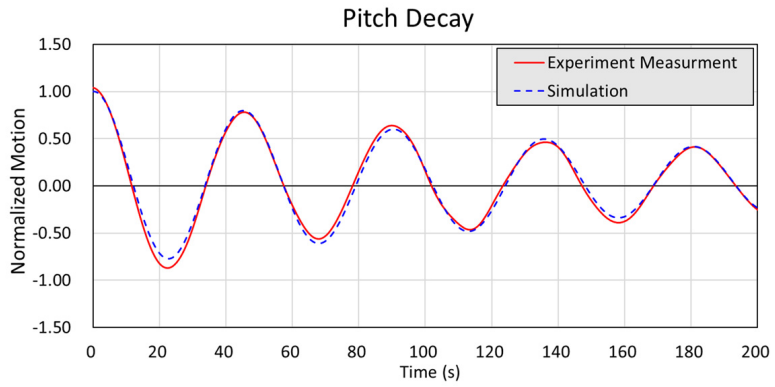

Figure 14. Comparison of time series between experiment and simulation result for pitch decay test.

4.2. Regular Wave Test

To investigate the six-degrees-of-freedom motion characteristics of K-Semi, a model test under regular waves. The test included 10 different periods, each with a wave height of 5 m and 180° incident wave. Details of this condition in full scale are presented in Table 3. The measured motion response of the model test was normalized with respect to the height of the incident wave to obtain the RAO under the incident wave period condition. A comparison between the results of the model test and those of the numerical analysis, both in the time and frequency domains, for the surge, heave, and pitch motions are presented in Figures 15–17. AdFlow was used for the frequency domain analysis, whereas the time–domain analysis was the result of the original and truncated mooring systems based on the numerical model using damping results from Section 4.1.

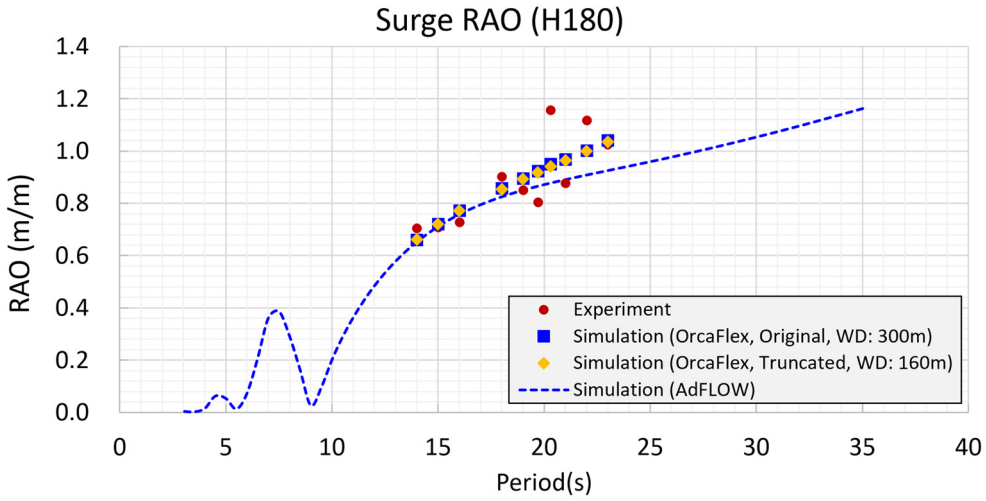

Figure 15. Surge RAO comparison between experiment and simulation.

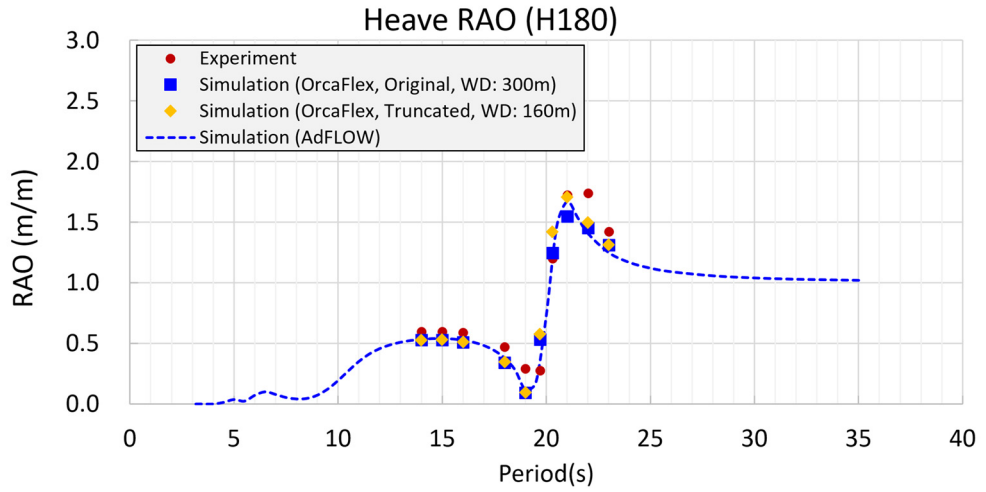

Figure 16. Heave RAO comparison between experiment and simulation.

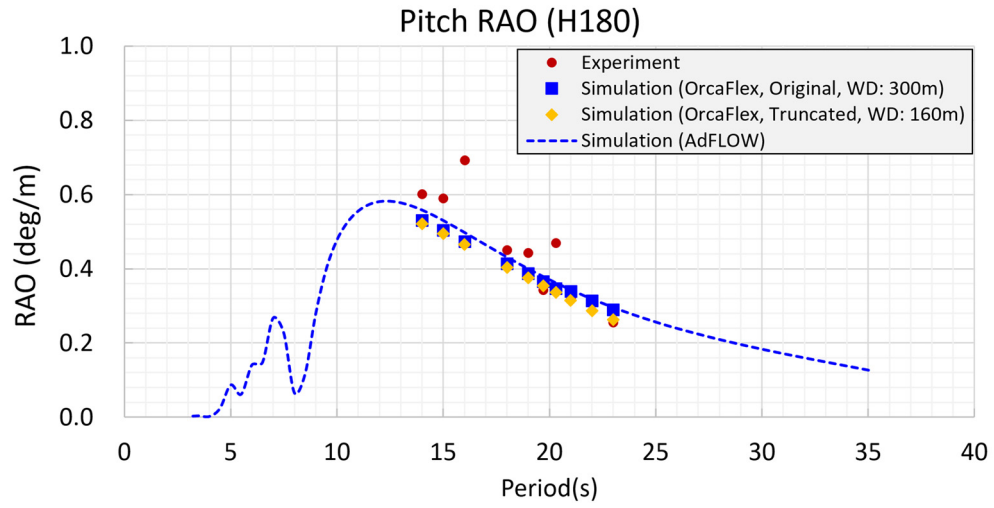

Figure 17. Pitch RAO comparison between experiment and simulation.

In summary, the results of the RAO, the model test, frequency-domain analysis, and time–domain analysis are similar. In particular, there was no significant difference in the RAO between the analysis results of the original and truncated mooring systems. The

objective of the regular wave test was to investigate the motion characteristics of the K-Semi under specific wave period conditions of the incident wave. In the test, there was no significant offset in the surge direction. Consequently, the variations in the motion characteristics owing to the variations in the heave restoring force and pitch restoring moment of the original and truncated mooring systems were not significant. However, in the case of the occurrence of a low-frequency drift motion, leading to a large offset in the wave direction, the variation in the heave restoring force and pitch restoring will increase, which may affect the motion characteristics of the K-Semi.

4.3. Low-Frequency Pitch Motion by Second-Order Wave Force

Semi-submersible offshore structures have the advantage of excellent motion performance due to their small waterplane areas. In the case of K-Semi, the natural period of the heave motion is approximately 20 s, whereas the natural period of roll and pitch motions is approximately 45 s. These periods are advantageous in avoiding resonance in the 10–20 s region, where wave energy is predominantly distributed. Therefore, excellent motion performance can be expected for the K-Semi because of the avoidance of the resonance region.

The horizontal motion of a moored floating body is characterized by a long natural period, principally due to the mooring system. The motion is mainly influenced by the second-order components of the waves—the mean drift force and second-order wave drift force. For ship-shaped offshore structures, the period of the roll motion is less than 20 s. Hence, the influence of these low-frequency nonlinear waves is minimal. However, some structures with longer natural periods are known to be influenced by second-order wave components. Similarly, because the natural periods of the roll and pitch motions were greater than 45 s, these motions of a semi-submersible were expected to be affected by the second-order components of the waves. These effects can be investigated by calculating the second-order pitch moment spectrum in Equation (1) using the QTF and the wave spectrum. The spectral density of the second-order motion can be calculated using Equation (2), and the standard deviation of the pitch motion due to the nonlinear wave component can be derived from Equation (3) [21].

The left-hand side of Figure 18 shows the QTF analysis result of the second-order wave force for the pitch motion of K-Semi using AdFlow, and the right-hand side shows the low-frequency pitch moment spectral density result of K-Semi obtained using Equation (2). Figure 19 shows the results of the low-frequency pitch motion spectral density calculation before integrating the right-hand side of Equation (3) and the wave spectrum of the irregular wave condition in the K-semi-model test. According to Figure 19, the wave energy was concentrated at approximately 0.59 rad/s (10.64 s), which was the period condition of the incident wave used in the irregular wave model test. However, the secondary pitch motion appeared at approximately 0.14 rad/s (for approximately 45 s), which is the low-frequency region with no wave energy. This result indicates that K-Semi exhibits a characteristic low-frequency behavior driven by the second-order wave force of the wave.

$$S_{m_y}^{(2)}(\mu) = 8\int_0^\infty S_w(\omega)S_w(\omega+\mu)M_y^{(2)}(\omega)M_y^{(2)}(\omega+\mu)d\omega \tag{1}$$

$$S_r(\omega) = \frac{S_{m_y}(\omega)}{\left(K_{55} - M_{55}\omega^2\right)^2 + C_{55}^2\omega^2} \tag{2}$$

$$\sigma_{pitch}^2 = \int_0^\infty \frac{S_{m_y}(\omega)}{\left(K_{55} - M_{55}\omega^2\right)^2 + C_{55}^2\omega^2}d\omega \tag{3}$$

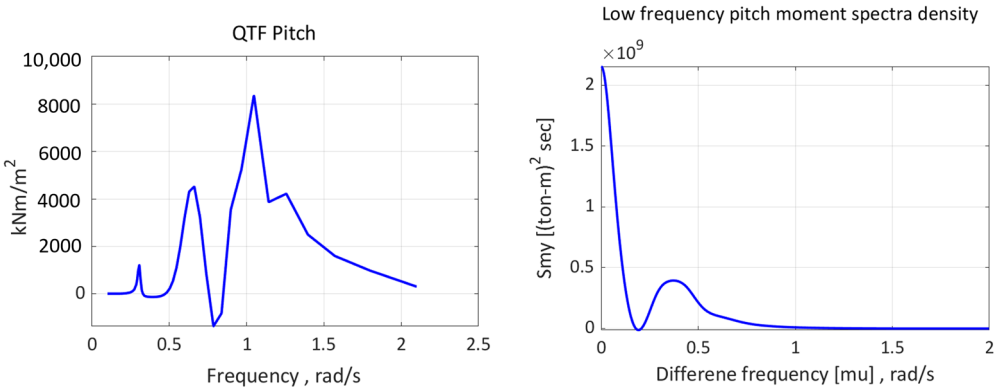

Figure 18. QTF of pitch motion (**left**)and pitch moment spectra density (**right**).

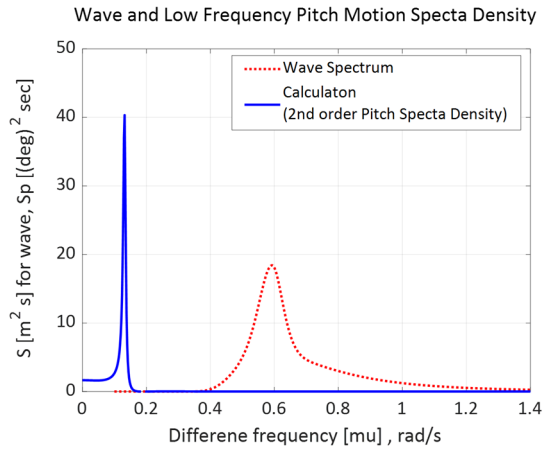

Figure 19. Spectra density of 2nd order pitch motion and wave spectrum of incident wave.

4.4. Irregular Wave Test

In order to investigate the motion response with truncated mooring, the model test of the K-semi was performed under the irregular wave conditions listed in Table 3 in the arrangement shown in Figure 8. Figures 20 and 21 show photographs of the model tests conducted in the DOEB. The measurement time was set to 3 h at full scale, and the motion characteristics of the K-Semi connected to the truncated mooring system were investigated based on the measured six-degrees-of-freedom motion results.

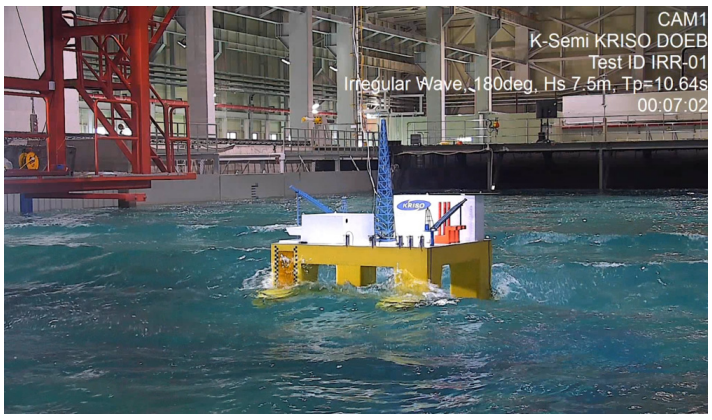

Figure 20. Snapshot of irregular wave model test (Side view).

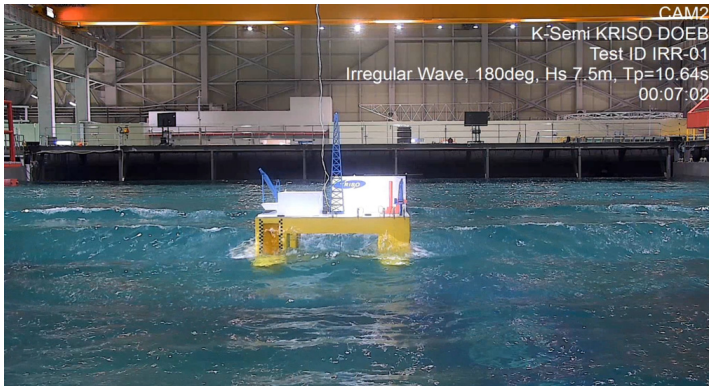

Figure 21. Snapshot of irregular wave model test (Front view).

Figure 22 shows the full-scale results of the time series of the surge, heave, and pitch motion measurements obtained from the model test. The findings show that the low-frequency surge motion is substantial, where the K-Semi moves up to −40 m from its initial position. Because of the large surge motion of the K-Semi, there is a large variation in the vertical restoration of the mooring system, as shown in Figures 10 and 11. Consequently, it is expected to affect the pitch motion characteristics of the K-Semi. This is evident in Figure 23, which shows the motion response spectra for surge and pitch motions. The motion response spectrum is shown in Figure 23. In the motion response spectrum, the low-frequency component of the surge motion is large, and the pitch response spectrum is characterized by three peaks. The first peak corresponds to the period of the incident wave at about 0.59 rad/s (10.64 s), and the second peak corresponds to the second-order pitch motion region at about 0.14 rad/s (greater than about 45 s). Figure 24 shows the second-order pitch motion spectrum calculated using Equation (3) and also the model test pitch motion spectrum results. The second-order pitch motion of the model test was in good agreement with the low-frequency pitch motion results calculated by the QTF, confirming the presence of the second-order pitch motion of the K-Semi.

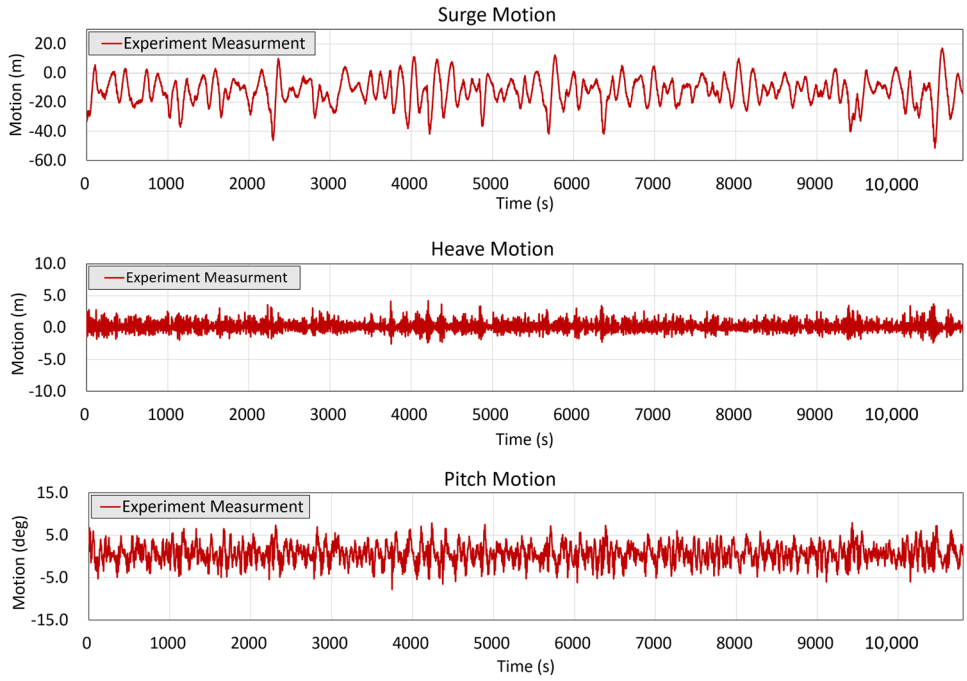

Figure 22. Time series results of surge, heave and pitch motion from irregular wave experiment.

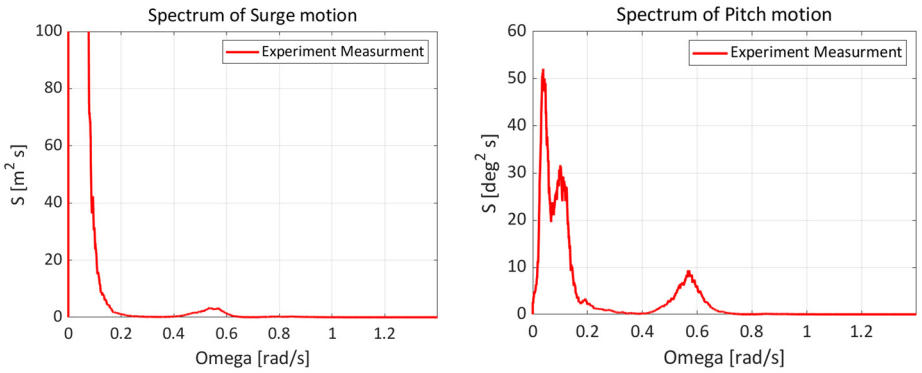

Figure 23. Motion spectrum of surge (**left**) and pitch (**right**) from model test.

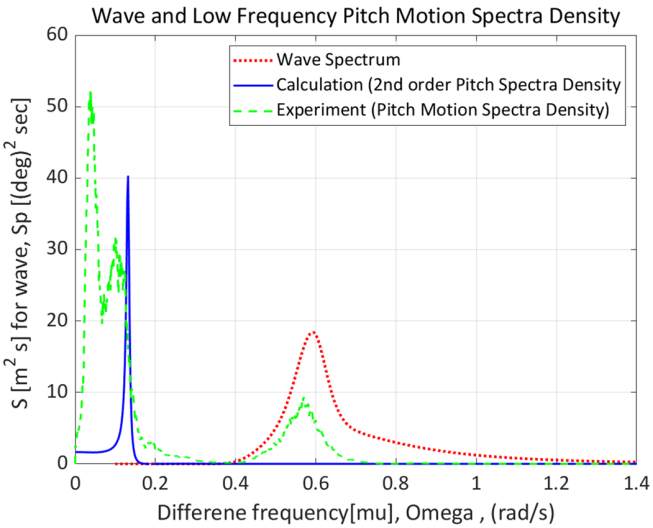

Figure 24. Response spectrum of pitch motion from model test and analysis.

The peak region below 0.08 rad/s (over 78.5 s) corresponds to the lowest frequency pitch motion component, which has a longer period than the second-order pitch motion component. This is close to the period of low-frequency drift motion in the surge direction. When large surges occur, the low-frequency pitch motions are large due to the difference in the restoring force between the front and rear ends of the mooring system connected to the K-Semi as well as the pitch moment. From the time series results shown in Figure 25, it is clear that the experiment shows an instantaneous increase in the surge due to the low-frequency surge motions caused by second-order low-frequency wave force, with a simultaneous large pitch motion. The tension results of the mooring line measured in the model test show the cause of coupling with surge and pitch motion. The mooring configuration in Figure 8 shows mooring line 4 connected in the bow direction and mooring line 9 connected in the stern direction of the K-Semi. In Figure 25, the line tension on mooring line 4 becomes larger while the load on mooring line 9 becomes smaller when the surge occurs. This asymmetry of load acts as a pitch moment on the floater, and the pitch moment results in a large pitch motion.

To comprehend the pitch motion characteristics of the K-Semi, which was the primary focus of this study, a filter was applied to the pitch time-series results obtained from the model test to separate the time series under each major periodic condition, consequent to which, the response spectrum was obtained. A bandpass filter was applied to the measurement results, resulting in three separate regions: the resonance period of the surge motion, the resonance period of the pitch motion of the K-semi, and the period of the incident wave. The original time series and spectrum were then reconstructed by summing each periodic component to ensure that no signal was lost due to the application of the filter.

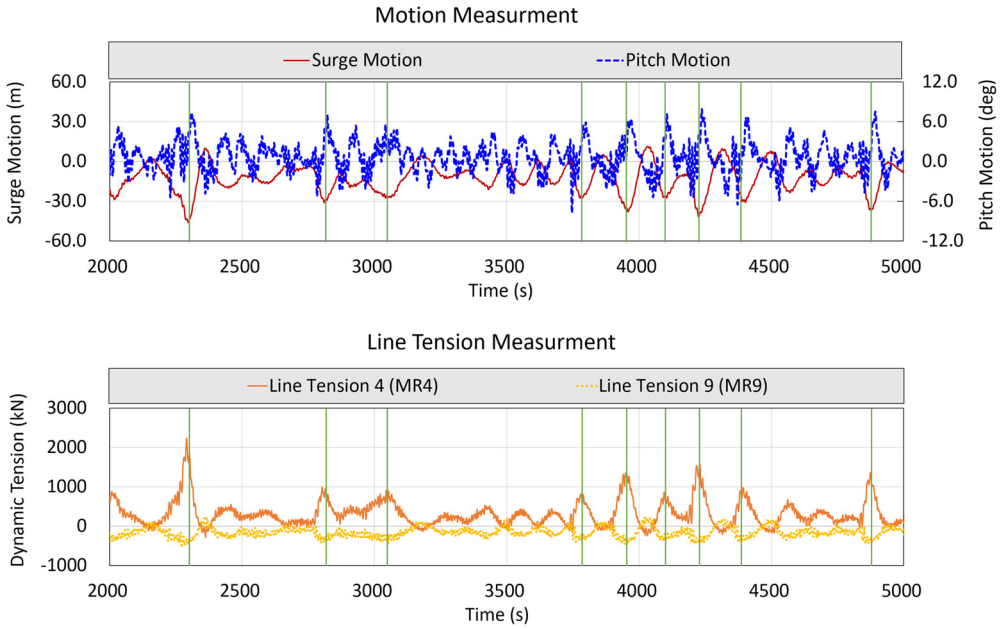

Figure 25. Time series results of motion and line tension for selected range from irregular wave experiment.

Figure 26 shows the time series of the truncated mooring model test with the motion components separated for each periodic condition after application of the filter. The response spectrum results are shown in Figure 27. These figures show that the pitch motion results of the model test exhibited three periodic condition components, as previously discussed.

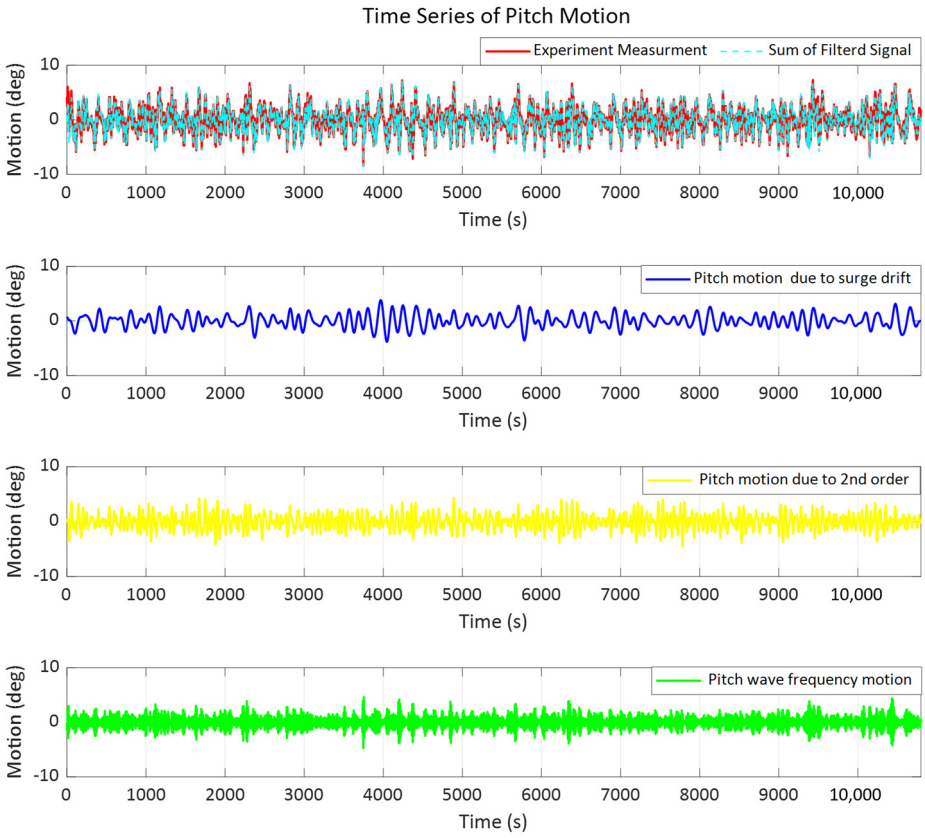

Figure 26. Raw and filtered time series of pitch motion for 3 different components from model test.

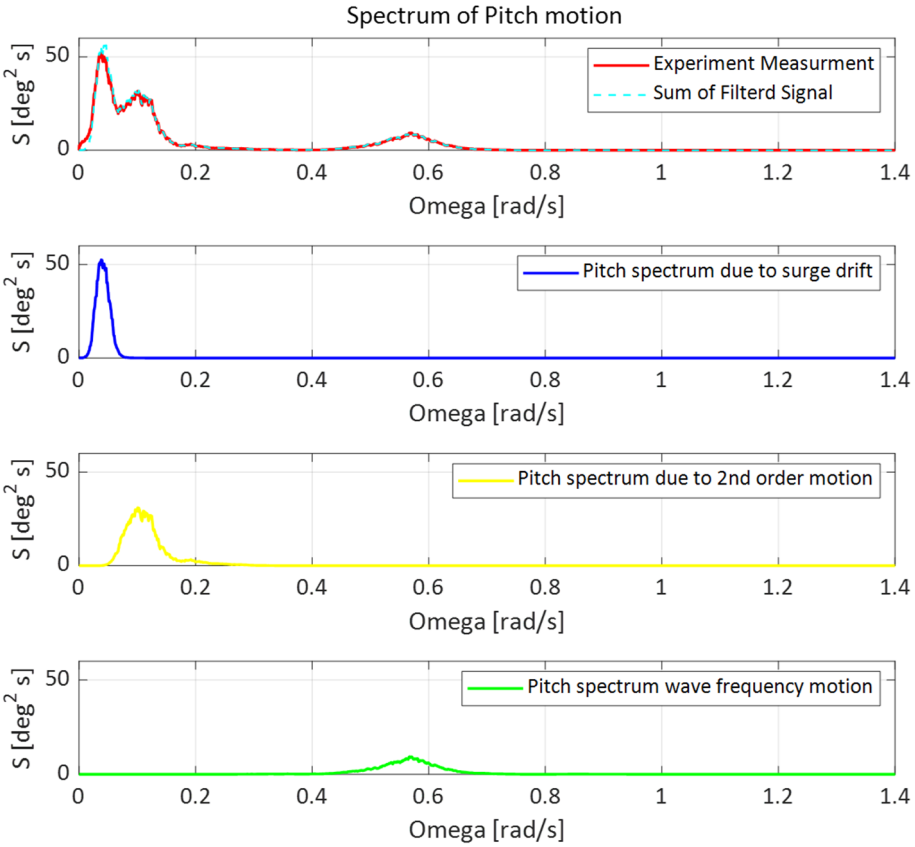

Figure 27. Raw and filtered response spectrum of pitch motion for 3 different components from model test.

Figure 28 presents a comparison between the results of the model test and numerical simulation for the surge, heave, and pitch motions. Previously, the numerical model was calibrated to show results similar to the time series of the decay test and the RAO of the regular wave test results. The numerical simulations showed a close resemblance to the results of the model test for the heave motion, whereas the results of the numerical simulation showed slight disagreement with the model test results for the surge and pitch motions. This is attributable to not accounting for the effect of the fluid drag component acting on the floating body, which increased the surge motion. Consequently, the smaller values obtained through the numerical results for the pitch motion, as compared to the model test, can be attributed to the diminished influence of the surge motion in the numerical simulation.

Figure 29 shows the response spectrum of the surge motion, indicating that the experiments and numerical simulations were similar in terms of the period over which the behavior occurred. Figure 30 shows a comparison of the response spectra for the pitch motion. Three peaks were observed in the experimental and numerical simulations. Under the periodic condition of the incident wave, about 0.59 rad/s (10.64 s), a linear motion owing to the incident wave was observed, and a long periodic motion was observed at about 0.14 rad/s (about 45 s or more), which is the second-order motion region. These are the same as the response spectrum using QTF in the frequency domain of Figure 19, which shows that the nonlinear motion due to nonlinear wave forces is significant in column structures such as K-Semi and is an important part of the performance evaluation of the motion response of the structure.

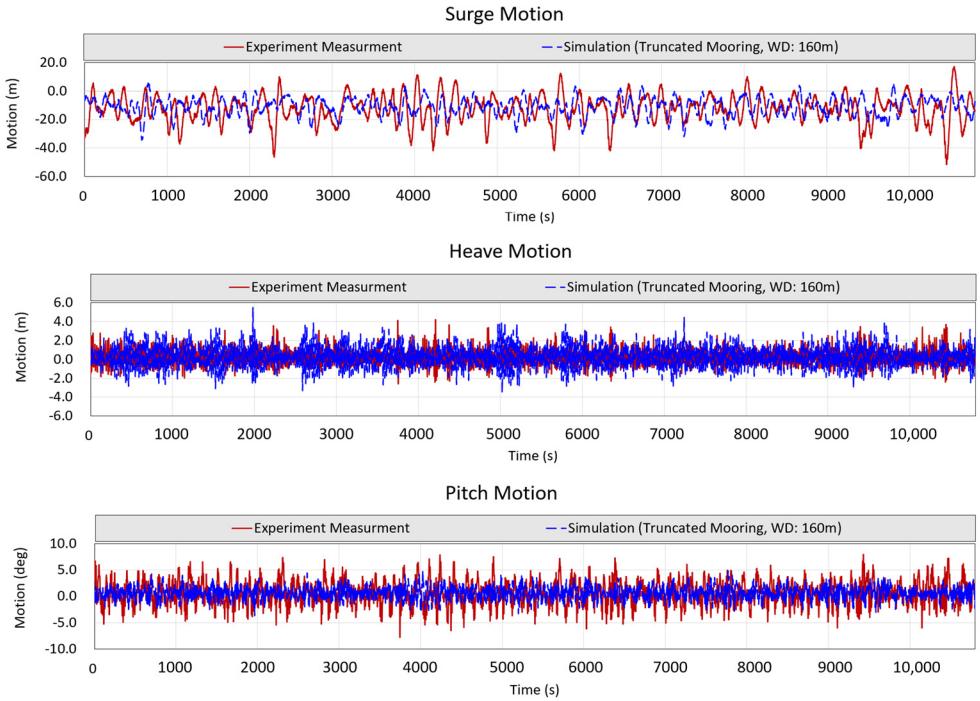

Figure 28. Comparison of time series of motions between model test and simulation of truncated mooring system.

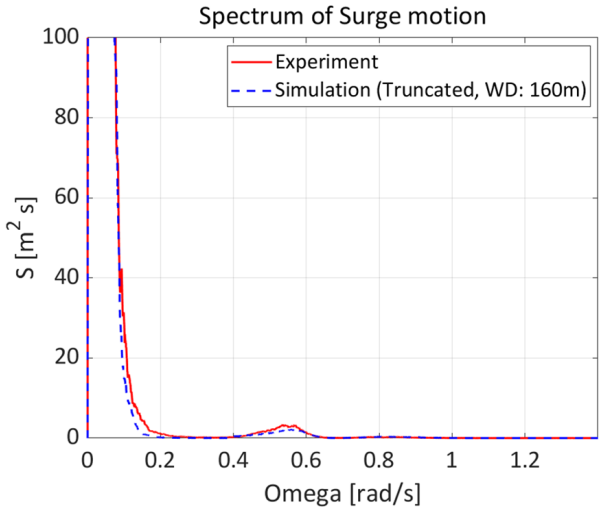

Figure 29. Comparison of response spectrum for surge between model test and simulation of truncated mooring system.

In addition, the lower frequency motion component compared to the second-order motion appears under the condition of 0.08 rad/s (more than 78.5 s), which corresponds to the natural period of the surge motion. In particular, the surge motion was large in the model test, which resulted in a large pitch motion. However, in the numerical analysis, as the surge motion was analyzed to be small, the effect on the pitch motion was also reduced, showing a relatively small result compared with the experiment. In the case of semi-submersible offshore structures such as K-Semi, it is necessary to investigate not only the position-keeping performance when the surge motion is large but also the excessive pitch motion associated with the surge motion and the relative wave height.

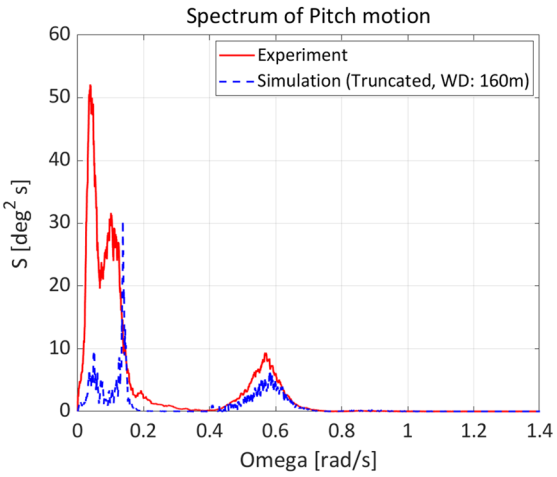

Figure 30. Comparison of response spectrum for pitch between model test and simulation of and truncated mooring system.

Figures 31 and 32 present the mean and standard deviations for each direction of motion. In the model test, surge motion showed a mean value of about −12.3 m, whereas smaller mean values of about −11.1 m resulted in the numerical simulations. However, the heave and pitch motions from the model test and simulation showed comparable results.

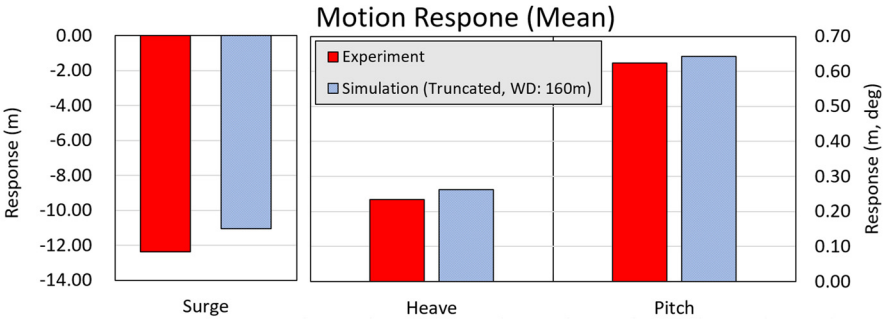

Figure 31. Mean value of surge, heave and pitch response of model test, simulation of original mooring system, and truncated mooring system.

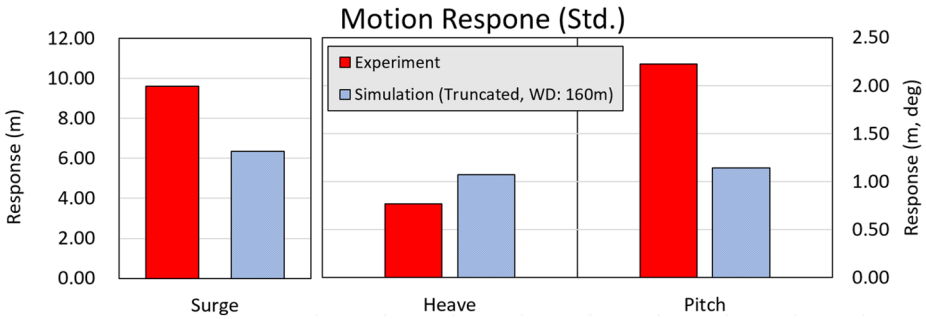

Figure 32. Standard deviation value of surge, heave and pitch response of model test, simulation of original mooring system, and truncated mooring system.

The standard deviation was utilized as a statistical parameter to indicate the motion characteristics and magnitude of the K-Semi, which is shown in Figure 32. The surge motion had the largest value in the experiment, whereas the heave motion had comparable results in both the model test and the numerical simulation. For the pitch motion, the model experiment showed a result of approximately 2.2°, whereas the numerical simulation showed results of approximately 1.2° for the truncated mooring. Smaller results for the pitch motion may be attributed to improper evaluation of the effects of the fluid drag

component of the floating body and mooring owing to the long-period surge motion in the simulation.

Figure 33 shows the standard deviation results of the model test and numerical simulation of the pitch motion divided into three main frequency components. As shown in Figure 33, the pitch motion in the model test and simulation can be divided into three components: the wave component, pitch motion due to second-order wave forces, and low-frequency pitch motion component associated with the surge motion. The effects of the surge drift motion and second-order wave forces on the pitch were similarly large, followed by the wave frequency component in the model test. The wave frequency component was approximately 1.0°, the second-order pitch motion was approximately 1.4°, and the pitch motion owing to the surge motion was approximately 1.2°, indicating that each component contributed evenly to the overall response. In the numerical analysis, three different frequency components were found, similar to the model test. However, their magnitudes were smaller than those in the model test. In the numerical analysis, the magnitude of the wave frequency component was approximately 70% of that of the model test. Additionally, the low-frequency motion component was approximately 40% or less.

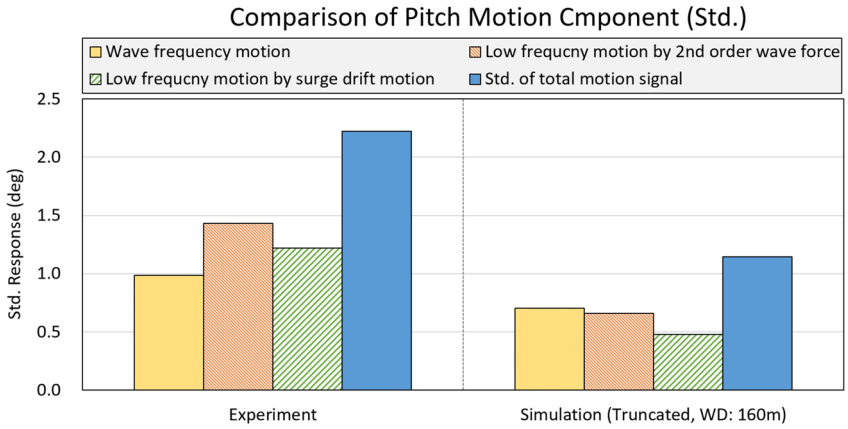

Figure 33. Comparison of standard deviation of each component for pitch response.

Although there are discrepancies between the model test and simulation results, it is confirmed that the results of the model test and simulation with the truncated mooring system are similar and show the three periodic components of the pitch motion due to the coupling phenomenon between the surge and pitch motion.

5. Conclusions

In this study, K-Semi, a KRISO standard offshore structure, was used as the target offshore structure to evaluate its motion characteristics with a truncated mooring system through a model test in the DOEB in Busan, Korea. The results were compared with the frequency domain and time domain numerical analysis.

Model tests were conducted using a 1:50 scale model, and the truncated mooring system was redesigned to suit the environment of an offshore basin. The numerical model was calibrated to verify its accuracy based on the results of the free decay and regular wave model tests. In addition, the motion response of the K-Semi under irregular waves was evaluated based on the motion measurement and numerical simulation results to investigate the motion characteristics of the K-Semi, a type of column structure.

The spectral analysis of the motion signal measured using the model test showed that there were three peaks. The frequency component of the incident wave was approximately 0.59 rad/s (10.64 s), the second-order pitch motion was approximately 0.14 rad/s (more than approximately 45 s), and the frequency component lower than the second-order component was approximately 0.08 rad/s (more than about 78.5 s). It is observed that the significant low-frequency pitch motion associated with the surge drift motion is caused by the restoring moment as well as the difference in the restoring force of the front and rear

ends of the mooring system connected to the K-Semi, as it experienced a large surge drift motion. The low-frequency pitch motion is influenced by the low-frequency surge motion because the pitch motion occurs significantly when the K-Semi shows a large surge motion, whereas the pitch motion at low frequencies is related to the frequency range of the surge motion.

The results of the numerical simulation were similar to those of the model test. Although the results of the model test and numerical simulation were comparable for the heave motion, the results of the numerical simulation were slightly lower for the surge and pitch motions. In particular, the numerical simulation results were smaller for surge motion. It is believed that the effect of the fluid drag component acting on the floating body was not included in the numerical simulation in this study, and it is expected that more accurate results would be obtained if it were included.

DNG-GL-OTG13 provides an efficient estimation method for wave impact and air gap assessment. DNV-GL-OTG13 takes into account the wave frequency upwell and low-frequency upwell components in evaluating the upwell phenomenon. It emphasizes the significance of considering the influence of the low-frequency motion component in these assessments. Pan et al. [22] mention that for a pontoon-type structure such as a semi-submersible with a long natural period, these low-frequency components should be fully considered in the heave, roll and pitch motions.

The pitch motion characteristics of the K-Semi under the irregular wave condition in the head sea condition were investigated by model test and numerical analysis for a column-type structure with small restoring coefficients in the vertical direction. The study revealed the significant impact of the low-frequency component caused by the surge motion, in addition to the wave frequency upwell and the second-order low-frequency motion component arising from the second-order wave force. Hence, when estimating the relative wave height of a pontoon-like structure, such as the K-Semi, it is necessary to consider the influence of the low-frequency component due to the surge motion of the floating body with the mooring system, as well as the second-order component to derive a rigorous upwell result.

Author Contributions: Conceptualization, B.P.; Methodology, B.P., S.J. and M.-G.S.; Software, B.P.; Validation, S.J. and M.-G.S.; Formal analysis, S.J.; Resources, J.K. and H.G.S.; Data curation, M.-G.S.; Writing—original draft, B.P.; Writing—review & editing, J.-C.P.; Supervision, B.P., J.K., H.G.S. and J.-C.P.; Project administration, J.K. All authors have read and agreed to the published version of the manuscript.

Funding: This research was supported by a grant from the Endowment Project for "Development of offshore green hydrogen production and storage platform technology," funded by the Korea Research Institute of Ships and Ocean engineering (PES4806).

Institutional Review Board Statement: Not applicable.

Informed Consent Statement: Not applicable.

Data Availability Statement: Not applicable.

Conflicts of Interest: The authors declare no conflict of interest.

References

1. Park, D.M.; Nam, H.S.; Seo, M.G.; Cho, S.K.; Hong, S.Y. Model Test on motion and wave impact load of the K-Semi. In Proceedings of the Spring Workshop of the Korea Towing Tank Conference, Seoul, Republic of Korea, 16 April 2021. (In Korean)
2. Zhong, W.; Zhang, X.; Wan, D. Hydrodynamic characteristics of a 15 MW semi-submersible floating offshore wind turbine in freak waves. *Ocean. Eng.* **2023**, *283*, 115094. [CrossRef]
3. DNVGL. *DNVGL–OTG–13-Prediction of Air Gap for Column Stabilised Units*; DNVGL: Oslo, Norway, 2019.
4. Nam, H.S.; Park, D.M.; Cho, S.K.; Hong, S.Y. Analysis of Relative Wave Elevation around Semi-submersible Platform through Model Test: Focusing on Comparison of Wave Probe Characteristics. *J. Ocean. Eng. Technol.* **2022**, *36*, 1–10. [CrossRef]
5. Kim, N.W.; Nam, B.W.; Cho, Y.; Sung, H.G.; Hong, S.Y. Experimental Study of Wave Run-up on Semi-submersible Offshore Structures in Regular Waves. *J. Ocean. Eng. Technol.* **2014**, *28*, 6–11. (In Korean) [CrossRef]

6. Reig, M.A.; Pegalajar-Jurado, A.; Mendikoa, I.; Petuya, V.; Bredmose, H. Accelerated second-order hydrodynamic load calculation on semi-submersible floaters. *Mar. Struct.* **2023**, *90*, 103430. [CrossRef]
7. Cao, Q.; Xiao, L.; Guo, X.; Liu, M. Second-order responses of a conceptual semi-submersible 10 MW wind turbine using full quadratic transfer functions. *Renew. Energy* **2020**, *153*, 653–668. [CrossRef]
8. Jung, S.J.; Kwak, H.U.; Kim, N.W.; Jung, D.W.; Park, B.W.; Jung, J.S.; Kim, J.H. Truncated mooring test at 2 different water depth cases of deep ocean engineering basin. In Proceedings of the KAOSTS '22 Conference, T1301, Jeju, Republic of Korea, 2–4 June 2022. (In Korean)
9. Nam, B.W.; Seo, M.G.; Hong, S.Y. Numerical Simulation on the Slow-Drift Motion of a Semi-Submersible Platform Considering Mooring Effects. In Proceedings of the International Workshop on Water Waves and Floating Bodies, Seoul, Republic of Korea, 25–28 April 2021.
10. Ghafari, H.; Dardel, M. Parametric study of catenary mooring system on the dynamic response of the semi-submersible platform. *Ocean. Eng.* **2018**, *153*, 319–332. [CrossRef]
11. Kim, B.W.; Sung, H.G.; Kim, J.H.; Hong, S.Y. Comparison of linear spring and nonlinear FEM methods in dynamic coupled analysis of floating structure and mooring system. *J. Fluid Struct.* **2013**, *42*, 205–227. [CrossRef]
12. Matos, V.L.F.; Ribeiro, E.O.; Simos, A.N.; Sphaier, S.H. Full scale measurements and theoretical predictions of 2nd order pitch and roll slow motions of a semi-submersible. *J. Offshore Mech. Arct. Eng.* **2013**, *135*, 031106. [CrossRef]
13. Molins, C.; Trubat, P.; Gironella, X.; Campos, A. Design Optimization for a Truncated Catenary Mooring System for Scale Model Test. *J. Mar. Sci. Eng.* **2015**, *3*, 1362–1381. [CrossRef]
14. Ferreira, F.; Lages, E.; Afonso, S.; Lyra, P. Dynamic design optimization of an equivalent truncated mooring system. *Ocean. Eng.* **2016**, *122*, 186–201. [CrossRef]
15. Kim, Y.H.; Kim, B.W.; Cho, S.K. Study on Design of Truncated Mooring Line with Static Similarity in Model Test Basins. *J. Ocean. Eng. Technol.* **2017**, *31*, 257–265. [CrossRef]
16. Waals, O.J.; van Dijk, R.R.T. Truncation Methods for Deep Water Mooring Systems for a Catenary Moored FPSO and a Semi Taut Moored Semi Submergible. In Proceedings of the Deep Offshore Technology Conference, New Orleans, LA, USA, 30 November–2 December 2004.
17. Wang, H.; Ma, G.; Sun, L.; Kang, Z. Truncation Design and Model Testing of a Deepwater FPSO Mooring System. *J. Offshore Mech. Arct. Eng.* **2016**, *138*, 021603. [CrossRef]
18. Li, X.; Wei, H.; Xiao, L.; Cheng, Z.; Liu, M. Study on the effects of mooring system stiffness on air gap response. *Ocean. Eng.* **2021**, *239*, 109798. [CrossRef]
19. Choi, Y.R.; Hong, S.Y.; Choi, H.S. An analysis of second-order wave forces on floating bodies by using a higher-order boundary element method. *Ocean. Eng.* **2000**, *28*, 117–138. [CrossRef]
20. Orcina. *OrcaFlexManual*; Version 11.3d; Orcina Ltd.: Ulverston, UK, 2023.
21. Liu, Y. On Second Order Roll Motions of Ships. In Proceedings of the 22th International Conference on Ocean, Offshore and Arctic Engineering, OMAE2003, Cancunn, Mexico, 8–13 June 2003.
22. Pan, Z.; Vada, T.K.; Nestegård, A. Efficient calculation of low frequency motions for air-gap prediction. In Proceedings of the 37th International Conference on Ocean, Offshore and Arctic Engineering, OMAE 2018, Madrid, Spain, 17–22 June 2018.